

Neural Metric Learning for Fast End-to-End Relation Extraction

Tung Tran

Department of Computer Science
University of Kentucky
Lexington, KY, USA
tung.tran@uky.edu

Ramakanth Kavuluru

Division of Biomedical Informatics
University of Kentucky
Lexington, KY, USA
ramakanth.kavuluru@uky.edu

Abstract

Relation extraction (RE) is an indispensable information extraction task in several disciplines. RE models typically assume that named entity recognition (NER) is already performed in a previous step by another independent model. Several recent efforts, under the theme of *end-to-end* RE, seek to exploit inter-task correlations by modeling both NER and RE tasks jointly. Earlier work in this area commonly reduces the task to a table-filling problem wherein an additional expensive decoding step involving beam search is applied to obtain globally consistent cell labels. In efforts that do not employ table-filling, global optimization in the form of CRFs with Viterbi decoding for the NER component is still necessary for competitive performance. We introduce a novel neural architecture utilizing the table structure, based on repeated applications of 2D convolutions for pooling local dependency and metric-based features, without the need for global optimization. We validate our model on the ADE and CoNLL04 datasets for end-to-end RE and demonstrate $\approx 1\%$ gain (in F-score) over prior best results with training and testing times that are nearly four times faster — the latter highly advantageous for time-sensitive end user applications.

1 Introduction

Information extraction (IE) systems are fundamental to the automatic construction of knowledge bases and ontologies from unstructured text. While important, in and of themselves, these resulting resources can be harnessed to advance other important language understanding applications including knowledge discovery and question answering systems. Among IE tasks are named entity recognition (NER) and binary relation extraction (RE) which involve identifying named entities and relations among them, respectively.

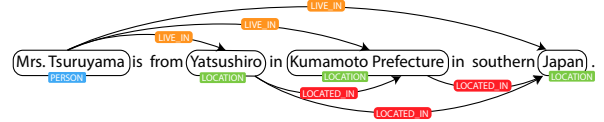


Figure 1: A simple relation extraction example.

We present Figure 1 as an example of the NER and RE problem given the input sentence “Mrs. Tsuruyama is from Yatsushiro in Kumamoto Prefecture in southern Japan.” First, we extract as entities the spans “Mrs. Tsuruyama”, “Yatsushiro”, “Kumamoto Prefecture”, and “Japan” where “Mrs. Tsuruyama” is of type PERSON and the rest are of type LOCATION. Thus, NER consists of identifying both the bounds and type of entities mentioned in the sentence. Once entities are identified, the next step is to extract relation triplets of the form (subject, predicate, object), if any, based on the context; for example, (Mrs. Tsuruyama, LIVE_IN, Yatsushiro) is a relation triple that may be extracted from the example sentence as output of an RE system.

NER and RE have been traditionally treated as independent problems to be solved separately and later combined in an ad-hoc manner as part of a pipeline system. End-to-end RE (E2ERE) is a relatively new research direction that seeks to model NER and RE jointly in a unified architecture. As these tasks are closely intertwined, joint models that simultaneously extract entities and their relations in a single framework have the capacity to exploit inter-task correlations and dependencies leading to potential performance gains. Moreover, joint approaches, like our method, are better equipped to handle datasets where entity annotations are non-exhaustive (that is, only entities involved in a relation are annotated), since standalone NER systems are not designed to handle incomplete annotations. Recent advancements in

deep learning for $\mathcal{E2ERE}$ are broadly divided into two categories: (1). The first category involves applying deep learning to the table structure first introduced by (Miwa and Sasaki, 2014), including Gupta et al. (2016), Pawar et al. (2017), and Zhang et al. (2017) where $\mathcal{E2ERE}$ is reduced to some variant of the table-filling problem such that the (i, j) -th cell is assigned a label that represents the relation between tokens at positions i and j in the sentence. Recent approaches based on the table structure operate on the idea that cell labels are dependent on features or predictions derived from preceding or adjacent cells; hence, the table is filled incrementally leading to potential efficiency issues. Also, these methods typically require an additional expensive decoding step, involving beam search, to obtain a globally optimal table-wide label assignment. (2). The second category includes models where NER and RE are modeled jointly with shared components or parameters without the table structure. Even state-of-the-art methods not utilizing the table structure rely on conditional random fields (CRFs) as an integral component of the NER subsystem where Viterbi algorithm is used to decode the best label assignment at test time (Bekoulis et al., 2018b,a).

Our model utilizes the table formulation by embedding features along the third dimension. We overcome efficiency issues by utilizing a more efficient and effective approach for deep feature aggregation such that local metric, dependency, and position based features are simultaneously pooled — in a 3×3 cellular window — over many applications of the 2D convolution. Intuitively, preliminary decisions are made at earlier layers and corroborated at later layers. Final label assignments for both NER and RE are made simultaneously via a simple *softmax* layer. In light of the recent success by Bekoulis et al. (2018a) in applying adversarial training (AT) to RE, we additionally explore AT as a regularization method for the proposed model. Thus, computationally, our model is expected to improve over earlier efforts without a costly decoding step. We validate our proposed method on the CoNLL04 dataset (Roth and Yih, 2004) and the ADE dataset (Gurulingappa et al., 2012), which correspond to the general English and the biomedical domain respectively, and show that our method improves over prior state-of-the-art in $\mathcal{E2ERE}$. We also show that our approach leads to training and testing times that are

four times faster, where the latter can be critical for time-sensitive end-user applications.

2 Related Work

Early efforts in $\mathcal{E2ERE}$ assume that entity bounds are given. In a seminal work, Roth and Yih (2004) proposed an integer linear programming (LP) approach to tackle the end-to-end problem. They discovered that the LP component was effective in enhancing classifier results by reducing semantic inconsistencies in the predictions compared to a traditional pipeline wherein the outputs of an NER component are passed as features into the RE component. Their results indicate that there are mutual inter-dependencies between NER and RE as subtasks which can be exploited. The LP technique has since been successfully applied in similar works (Choi et al., 2006; Kate and Mooney, 2010). Other efforts include the use of a probabilistic graphical model (Yu and Lam, 2010; Singh et al., 2013) and CRF-based joint inference model (Yang and Cardie, 2013).

Li and Ji (2014) proposed one of the first truly joint models wherein entities, including entity mention bounds, and their relations are predicted. Structured perceptrons (Collins, 2002), as a learning framework, are used to estimate feature weights while beam search is used to explore partial solutions to incrementally arrive at the most probable structure. Miwa and Sasaki (2014) proposed the idea of using a table representation which simplifies the task into a table-filling problem such that NER and relation labels are assigned to cells of the table; the aim was to predict the most probable label assignment to the table, out of all possible assignments, using beam search. While the representation is in table form, beam search is performed sequentially, one cell-assignment per step. The table-filling problem for $\mathcal{E2ERE}$ has since been successfully transferred to the deep neural network (DNN) setting (Gupta et al., 2016; Pawar et al., 2017; Zhang et al., 2017).

Other recent approaches not utilizing a table structure include modeling the entity and relation extraction task jointly with shared parameters (Miwa and Bansal, 2016; Li et al., 2016; Zheng et al., 2017a; Li et al., 2017; Katiyar and Cardie, 2017; Bekoulis et al., 2018b; Zeng et al., 2018). Katiyar and Cardie (2017) and Bekoulis et al. (2018b) specifically use attention mechanisms for the RE component without the need for

dependency parse features. Zheng et al. (2017b) operate by reducing the problem to a sequence-labeling task that relies on a novel tagging scheme. Zeng et al. (2018) use an encoder-decoder network such that the input sentence is encoded as fixed-length vector and decoded to relation triples directly. Most recently, Bekoulis et al. (2018a) found that adversarial training (AT) is an effective regularization approach for $\mathcal{E}2\mathcal{E}RE$ performance.

3 Method

We present our version of the table-filling problem, a novel neural network architecture to fill the table, and details of the training process.

3.1 The Table-Filling Problem

Intuitively, given a sentence of length n , we use an $n \times n$ table to represent a set of semantic relations such that the (i, j) -th cell represents the relationship (or non-relation) between tokens i and j . In practice, we assign a tag for each cell in the table such that entity tags are encoded along the diagonal while relation tags are encoded at non-diagonal cells. For entity recognition, we use the BILOU tagging scheme (Ratinov and Roth, 2009). In the BILOU scheme, B , I , and L tags are used to indicate the beginning, inside, and last token of a multi-token entity respectively. The O tag is used to indicate whether the token outside of an entity span, and U is used for unit-length entities.

In tabular form, entity and relation tags are drawn from a unified list \mathcal{Z} serving as the label space; that is, each cell in the table is assigned exactly one tag from \mathcal{Z} . For simplicity, the O tag is also used to indicate a *null* relation when occurring outside of a diagonal. As each entity type requires a BILOU variant, a problem with n_{ent} entity types and n_{rel} relation types has $|\mathcal{Z}| = 4n_{\text{ent}} + n_{\text{rel}} + 1$ where the last term accounts for the O tag. Our conception of the table-filling problem differs from Miwa and Sasaki (2014) in that we utilize the entire table as opposed to only the lower triangle; this allows us to model directed relations without the need for additional inverse-relation tags. Moreover, we assign relation tags to cells where entity spans intersect instead of where head words intersect; thus encoded relations manifest as rectangular blocks in the proposed table representation. We present a visualization of our table representation in Figure 2. At test time, entities are first extracted, and relations are subse-

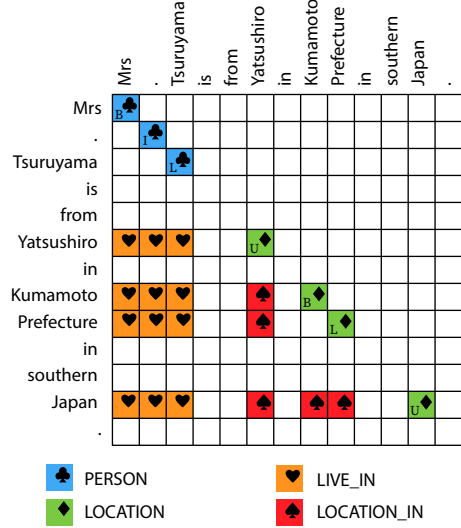


Figure 2: Table representation for the example in Figure 1. BILOU-encoded entity tags are assigned along the diagonal and relation tags are assigned where entity spans intersect. Empty cells are implicitly assigned the O tag.

quently extracted by averaging the output probability estimates of the blocks where entities intersect. We describe the exact procedure for extracting relations from these blocks at test-time in Section 3.3.

3.2 Our Model: Relation-Metric Network

We propose a novel neural architecture, which we call the relation-metric network, combining the ideas of metric learning and convolutional neural networks (CNNs) for table filling. The schematic of the network is shown in Figure 3, whose components will be detailed in this section.

3.2.1 Context Embeddings Layer

In addition to word embeddings, we employ character-CNN based representations as commonly observed in recent neural NER models (Chiu and Nichols, 2016) and $\mathcal{E}2\mathcal{E}RE$ models (Li et al., 2017). For the proposed model, such representations are composed by convolving over character embeddings of size π using a window of size 3, producing η feature maps; the feature maps are then max-pooled to produce η -length feature representations. As our approach is standard, we refer readers to Chiu and Nichols (2016) for full details. This portion of the network is illustrated in step ① of Figure 3.

Suppose the input is a sentence of length n represented by a sequence of word indices w_1, \dots, w_n into the vocabulary $\mathcal{V}^{\text{Word}}$ and an as-

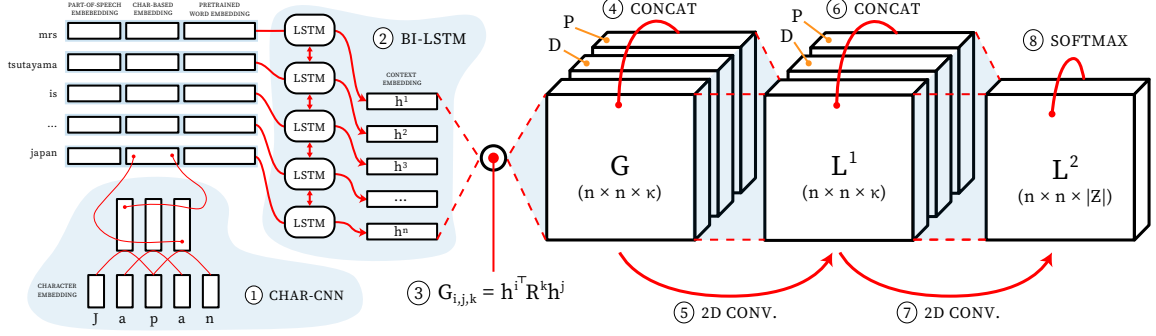


Figure 3: Overview of the network architecture for $\lambda = 2$. For simplicity, we ignore punctuation tokens.

sociated sequence of Part-of-Speech (PoS) tag indices p_1, \dots, p_n into the vocabulary \mathcal{V}^{PoS} . Each word and PoS tag is mapped to an embedding vector via embedding matrices $E^{\text{Word}} \in \mathbb{R}^{|\mathcal{V}^{\text{Word}}| \times \delta}$ and $E^{\text{PoS}} \in \mathbb{R}^{|\mathcal{V}^{\text{PoS}}| \times \mu}$ respectively such that δ and μ are hyperparameters that determine the size of the embeddings. Next, let $C[i]$ be the character-based representation for the i^{th} word. An input sentence is represented by matrix S wherein rows are words mapped to their corresponding embedding vectors; or concretely,

$$S = \begin{pmatrix} E^{\text{PoS}}[p_1] \parallel E^{\text{Word}}[w_1] \parallel C[1] \\ \vdots \\ E^{\text{PoS}}[p_n] \parallel E^{\text{Word}}[w_n] \parallel C[n] \end{pmatrix}$$

where \parallel is the vector concatenation operator, $E^{\text{PoS}}[i]$ is the i^{th} row of E^{PoS} and $E^{\text{Word}}[i]$ is the i^{th} row of E^{Word} .

Next, we compose *context* embedding vectors (CVs), which embed each word of the sentence with additional contextual features. Suppose $\overrightarrow{\text{LSTM}}$ and $\overleftarrow{\text{LSTM}}$ represent LSTM composition in the forward and backward direction, respectively, and let ρ be a hyperparameter that determines context embedding size. We feed S to a Bi-LSTM layer of hidden unit size $\frac{1}{2}\rho$ such that $\overrightarrow{\mathbf{h}}^i = \overrightarrow{\text{LSTM}}(S[i])$, $\overleftarrow{\mathbf{h}}^i = \overleftarrow{\text{LSTM}}(S[i])$, and $\mathbf{h}^i = \overrightarrow{\mathbf{h}}^i \parallel \overleftarrow{\mathbf{h}}^i$, for $i = 1, \dots, n$, where $S[i]$ is the i^{th} row of S and $\mathbf{h}^i \in \mathbb{R}^\rho$ represents the context centered at the i^{th} word. The output of the Bi-LSTM can be represented as a matrix $H \in \mathbb{R}^{n \times \rho}$ such that $H = (\mathbf{h}^1, \dots, \mathbf{h}^n)^\top$. This concludes step ② of Figure 3.

3.2.2 Relation-Metric Learning

Our goal is to design a network such that any two CVs can be compared via some “relatedness” measure; that is, we wish to learn a relatedness measure (as a parameterized function) that is able

to capture correlative features indicating semantic relationships. A common approach in metric learning to parameterize a relatedness function is to model it in bilinear form. Here for RE, for input CVs $\mathbf{x}, \mathbf{z} \in \mathbb{R}^m$, a relatedness function in bilinear form is similarly defined as $s_R(\mathbf{x}, \mathbf{z}) = \mathbf{x}^\top R \mathbf{z}$, where $R \in \mathbb{R}^{m \times m}$ is a parameter of the relatedness function, dubbed a *relation-metric embedding* matrix, learned during the training process.

Our aim is to compute s_R for all pairs of CVs in the sentence. Concretely, we can compute a “relational-metric table” $G \in \mathbb{R}^{n \times n}$ over all pairs of CVs in the sentence such that $G_{i,j} = \mathbf{h}^i^\top R \mathbf{h}^j$. In fact, we can learn a collection of κ similarity functions corresponding to κ relation metric tables; for our purposes, this is analogous to learning a diverse set of convolution filters in the context of CNNs. Thus we have the 3-dimensional tensor

$$G_{i,j,k} = \mathbf{h}^i^\top R^k \mathbf{h}^j, \quad \text{for } k = 1, \dots, \kappa, \quad (1)$$

with $G \in \mathbb{R}^{n \times n \times \kappa}$ where the first and second dimension correspond to word position indices while the third dimension embeds metric-based features. This constitutes step ③ of Figure 3. We show how G is consumed by the rest of the network in Section 3.2.6. However, as a prerequisite, we first describe how dependency parse and relative position information is prepared in Section 3.2.3 and Section 3.2.4 respectively and define the 2D convolution in Section 3.2.5.

3.2.3 Dependency Embeddings Table

Let \mathcal{V}^{dep} be the vocabulary of syntactic dependency tags (e.g., *nsubj*, *doj*). For an input sentence, let $\mathcal{T} = \{(a_1, b_1, z_1), \dots, (a_{\hat{d}}, b_{\hat{d}}, z_{\hat{d}})\}$ be the set of dependency relations where z_i are mappings to tags in \mathcal{V}^{dep} that express the dependency-based relations between pairs of words at positions $a_i, b_i \in \{1, \dots, n\}$, respectively. We define the dependency embedding ma-

trix as $F^{\text{dep}} \in \mathbb{R}^{|\mathcal{V}^{\text{dep}}| \times \beta}$, where each unique dependency tag is a β -dimensional embedding. We compose the dependency representation tensor D for \mathcal{T} as

$$D_{i,j,k} = \begin{cases} F_{t,k}^{\text{dep}} & \text{if } (i,j,t) \in \mathcal{T} \text{ or } (j,i,t) \in \mathcal{T}, \\ \phi_k & \text{otherwise,} \end{cases}$$

for $k = 1, \dots, \beta$, where ϕ is a trainable embedding vector representing the *null* dependency relation. As shown in the above equation for $D_{i,j,k}$, we embed the dependency parse tree simply as an undirected graph.

3.2.4 Position Embeddings Table

First proposed by Zeng et al. (2014), so called *position vectors* have been shown to be effective in neural models for relation classification. Position vectors are designed to encode the relative offset between a word and the two candidate entities (for RE) as fixed-length embeddings. We bring this idea to the tabular setting by proposing a *position* embeddings table P , which is composed the same way as the dependencies table; however, instead of dependency tags, we simply encode the distance between two candidate CVs as discrete labels mapped to fixed-length embeddings (of size γ , a hyperparameter). It is straightforward to see there will be $2(n_{\max} - 1) + 1$ distinct position offset labels where n_{\max} is the maximum length of a sentence in the training data. Both dependency and position embedding tensors are concatenated to the metric tensor (Eq. (1)) along the 3rd dimension prior to every convolution operation. Hence they are shown in steps (4) and (6) of Figure 3 for the network with two convolutional layers.

3.2.5 2D Convolution Operation

Unlike the standard 2D convolution typically used in NLP tasks, which takes 2D input, our 2D convolution operates on 3D input commonly seen in computer vision tasks where colored image data has height, width, and an additional dimension for color channel. The goal of the 2D convolution is to pool information within a 3×3 window along the first two dimensions such that metric features and dependency/positional information of adjacent cells are pooled locally over several layers. However, it is necessary to perform a *padded* convolution to ensure that dimensions corresponding to word positions are not altered by the convolution. We denote this padding transformation using the *hat* accent. That is, for some ten-

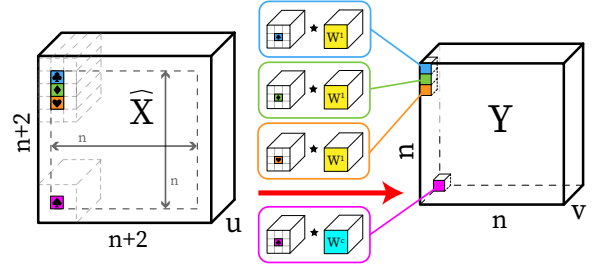


Figure 4: 2D convolution on 3D input with padding

sor input $X \in \mathbb{R}^{n \times n \times m}$, the padded version is $\hat{X} \in \mathbb{R}^{(n+2) \times (n+2) \times m}$ and the zero-padding exists at the beginning and at the end of the first and second dimensions. Next, we define the 2D convolution operation via the \star operator which corresponds to an element-wise product of two tensors followed by summation over the products; formally, for two input tensors A and B , $A \star B = \sum_i \sum_j \sum_k A_{i,j,k} B_{i,j,k}$.

Now our 2D convolution step is a tensor map $f_v(X) : \mathbb{R}^{n \times n \times u} \rightarrow \mathbb{R}^{n \times n \times v}$ with v filters of size $3 \times 3 \times u$, defined as

$$f_v(X)_{i,j,k} = W^k \star \hat{X}_{[i:i+2][j:j+2][1:u]} + b^k \quad (2)$$

for $i = 1, \dots, n, j = 1, \dots, n, k = 1, \dots, v$, where $W^k \in \mathbb{R}^{3 \times 3 \times v}$ and $b^k \in \mathbb{R}^{3 \times 3}$ for $k = 1, \dots, v$, are filter variables and bias terms respectively, and $\hat{X}_{[i:i+2][j:j+2][1:u]}$ is a $3 \times 3 \times u$ window of \hat{X} from i to $i + 2$ along the first dimension, j to $j + 2$ along the second dimension, and 1 to u along the final dimension. We show how $f_v(X)$ is used to repeatedly pool contextual information in Section 3.2.6. Instead of a 3×3 window, the convolution operation can be over any $t \times t$ window for some odd $t \geq 3$ where large t values lead to larger parameter spaces and multiplication operations. The 2D convolution is illustrated in Figure 4 and manifests in steps (5) and (7) of Figure 3.

3.2.6 Pooling Mechanism

Central to our architecture is the iterative *pooling* mechanism designed so that preliminary decisions are made in early iterations and further corroborated in subsequent iterations. It also facilitates the propagation of local metric and dependency/positional features to neighboring cells. Let \mathcal{Z} be the set of tags for the target task. We denote hyper-parameters κ and λ as the number of channels and the number of CNN layers respectively, where κ is same hyperparameter previously defined to represent the size of metric-based features. The pooling layers are defined recursively

with base case $L^1 = \text{relu}(f_\kappa(G \parallel D \parallel P))$ and

$$L^i = \begin{cases} \text{relu}(f_\kappa(L^{i-1} \parallel D \parallel P)) & 1 < i < \lambda, \\ f_{|\mathcal{Z}|}(L^{i-1} \parallel D \parallel P) & i = \lambda, \end{cases}$$

where f is the convolution function from Eq. (2), G is the tensor from Eq. (1), and \parallel is the tensor concatenation operator along the third dimension, and $\text{relu}(x) = \max(0, x)$ is the linear rectifier activation function. Here, κ and λ determine the breadth and depth of the architecture. A higher λ corresponds to a larger receptive field when making final predictions. The last layer, L^λ , is the output layer immediately prior to application of the *softmax* function. Given the architecture in Figure 3 with two convolutional layers, the convolve-and-pool operation is applied twice, indicated as steps ⑤ and ⑦ in the figure.

3.2.7 Softmax Output Layer

Given L^λ , we apply the *softmax* function along the third dimension to obtain a categorical distribution tensor $Q \in \mathbb{R}^{n \times n \times |\mathcal{Z}|}$ over output tags \mathcal{Z} for each word position pair such that $Q_{i,j,k} = \exp(L_{i,j,k}^\lambda) / (\sum_{l=1}^{|\mathcal{Z}|} \exp(L_{i,j,l}^\lambda))$, where $Q_{i,j,k}$ is the probability estimate of the pair of words at position i and j being assigned the k th tag. This constitutes the final step ⑧ of the network (Figure 3). Suppose $Y \in \mathbb{R}^{n \times n \times |\mathcal{Z}|}$ represents the corresponding one-hot encoded groundtruth along the third dimension such that $Y_{i,j,k} \in \{0, 1\}$. Then the example-based loss ℓ is obtained by summing the categorical cross-entropy loss over each cell in the table, normalized by the number of words in the sentence; that is, $\ell(Y, Q; \theta) = -(1/n) \sum_{i=1}^n \sum_{j=1}^n \sum_{k=1}^{|\mathcal{Z}|} Y_{i,j,k} \log(Q_{i,j,k})$, where θ is the network parameter set. During training, the loss ℓ is computed per example and averaged along the mini-batch dimension.

3.3 Decoding

While we learn concrete tags during training, the process for extracting predictions is slightly more nuanced. Entity spans are straightforwardly extracted by decoding BIOES tags along the diagonal. However, RE is based on “ensembling” the cellular outputs of the table where entity spans intersect. For entities a and b represented by their starting and ending offsets, (a_S, a_E) and (b_S, b_E) , the relation between them is the label computed as $\arg\max_{1 \leq k \leq |\mathcal{Z}|} \sum_{i=a_S}^{a_E} \sum_{j=b_S}^{b_E} Q_{i,j,k}$, which indexes a tag in the label space \mathcal{Z} .

3.4 Adversarial Training (AT)

Goodfellow and Jones (2015) introduced adversarial training (AT) as a regularization strategy for deep learning beyond standard dropout. With AT, the idea is to generate new adversarial examples — these are difficult examples likely to be misclassified by the network — for training by applying the *worst-case perturbations* to existing examples. These perturbations are defined as changes to the input that maximizes the loss. Bekoulis et al. (2018a) showed that AT is highly effective for $\mathcal{E}2\mathcal{E}RE$. Given this, we apply AT to our model in a similar fashion with the goal of attaining similar performance gains. Unlike Bekoulis et al. (2018a), we generate adversarial examples at the relation-metric table level, corresponding to hidden representation G , instead of at the word embedding level. This approach is more computationally efficient for the proposed architecture given we bypass the earlier LSTM layers.

Let $\ell(G; \theta)$ denote the training loss given a relation-metric table G and a set of network weights θ . We learn the worst-case perturbation ϕ as

$$\phi = \arg\max_{\phi': \|\phi'\|_2 \leq \epsilon} \ell(G + \phi'; \hat{\theta})$$

where $\hat{\theta}$ is a copy of current parameters and ϵ is a hyperparameter. Since computing the exact value of ϕ is intractable, like prior works (Yasunaga et al., 2017; Bekoulis et al., 2018a), we use the approximation proposed by Goodfellow and Jones (2015) to compute ϕ via a single gradient computation such that $\phi = \epsilon g / \|g\|_2$ where $g = \Delta_G \ell(G; \hat{\theta})$. We set $\epsilon = \alpha \sqrt{\kappa}$ so that it is adaptive to the embedding-dimension of G . The generated adversarial example is then $G_{adv} = G + \phi$ where α is a new hyperparameter (subsuming ϵ) that configures the magnitude of the perturbation. We train on an original example and its adversarially generated version jointly while optimizing on the new adversarial loss $\ell_{adv} = \ell(G; \hat{\theta}) + \ell(G_{adv}; \hat{\theta})$.

4 Experimental Setup

We note that the computing hardware is controlled across experiments given we report training and testing run times. Specifically, we used the Amazon AWS EC2 p2.xlarge instance which sports the NVIDIA Tesla K80 GPU with 12 GB memory.

4.1 Evaluation Metrics

We use the well-known F1 measure to evaluate NER and RE subtasks as in prior work. For NER, a predicted entity is treated as a *true positive* if it is exactly matched to an entity in the groundtruth based on both character offsets and entity type. For RE, a predicted relation is treated as a *true positive* if it is exactly matched to a relation in the ground truth based on subject/object entities and relation type. Hence, relation extraction performance is directly dependent on NER performance.

4.2 Datasets

CoNLL04. We use the dataset originally released by Roth and Yih (2004) with 1441 examples consisting of news articles from outlets such as WSJ and AP. The dataset has four entity types including *Person*, *Location*, *Organization*, and *Other* and five relation types including *Live_In*, *Located_In*, *OrgBased_In*, *Work_For*, and *Kill*. We report results based on training/testing on the same train-test split as established by Gupta et al. (2016); Adel and Schütze (2017); Bekoulis et al. (2018b,a), which consists of 910 training, 243 development, and 288 testing instances.

ADE. We also validate our method on the Adverse Drug Events (ADE) dataset from Gurulingappa et al. (2012) for extracting drug-related adverse effects from medical text. Here, the only entity types are *Drug* and *Disease* and the relation extraction task is strictly binary (i.e., Yes/No w.r.t the ADE relation). The examples are divided in two partitions: the first partition of 6821 sentences contain at least one drug/disease pair while the second partition of 16695 sentences contain no drug/disease pairs. As with prior work (Li et al., 2016, 2017; Bekoulis et al., 2018b,a), we only use examples from the first partition from which 120 relations with nested entity annotations (such as “lithium intoxication” where *lithium* and *lithium intoxication* are the drug/disease pair) are removed. Since sentences are duplicated for each pair of drug/disease mention in the original dataset, when collapsed on *unique* sentences, the final dataset used in our experiments constitutes 4271 sentences in total. Given there are no official train-test splits, we report results based on 10-fold cross-validation, where results are based on averaging performance across the ten folds, as in prior work.

Setting	Value	Setting	Value
Optimization Method	RMSProp	π	25
Learning Rate	0.005	η	50
Dropout Rate	0.5	μ	25
Num. Epochs	100	γ	25
Num. Channels (κ)	15	β	10
Num. Layers (λ)	8	δ	200
Adversarial Training α	0.0001	ρ	200

Table 1: Model configuration as tuned on the CoNLL04 development set.

4.3 Model Configuration

We tuned our model on the CoNLL04 development set; the corresponding configuration of our model (including hyperparameter values) used in our main experiments is shown in Table 1. For the ADE dataset, we used Word2Vec embeddings pretrained on the corpus of PubMed abstracts (Pyysalo et al., 2013). For the CoNLL04 dataset, we used GloVe embeddings pretrained on Wikipedia and Gigaword (Pennington et al., 2014). All other variables are initialized using values drawn from a normal distribution with a mean of 0 and standard deviation of 0.1 and further tuned during training. Words were tokenized on both spaces and punctuations; punctuation tokens were kept as is common practice for NER systems. For part-of-speech and dependency parsing, we use SyntaxNet¹ which implements the transition-based neural model by Andor et al. (2016). We trained the aforementioned parser, using default settings, on the CoNLL 2017 corpus (Zeman et al., 2018) to obtain projective dependency parses for CoNLL04 examples. We used the GENIA corpus (Kim et al., 2003) to train and obtain projective dependency parses for ADE examples. Early experiments showed that exponential decay in conjunction with batch normalization is essential for stable/effective learning for this particular architecture. In terms of learning rate schedule, we apply exponential decay to the learning rate such that it is roughly halved every 10 epochs; concretely, $r_k = r_b^{\frac{k}{10}}$ where r_b is the base learning rate and r_k is the rate at the k th epoch. We apply dropout (Srivastava et al., 2014) on h_i for $i = 1, \dots, n$ as regularization at the earlier layers. However, dropout had a detrimental impact when applied to later layers. We instead apply batch-normalization (Ioffe and Szegedy, 2015) as a form of regularization on representations G and L^i for $i = 1, \dots, \lambda$. We use optimize the learning objec-

¹<https://github.com/tensorflow/models/tree/master/research/syntaxnet>

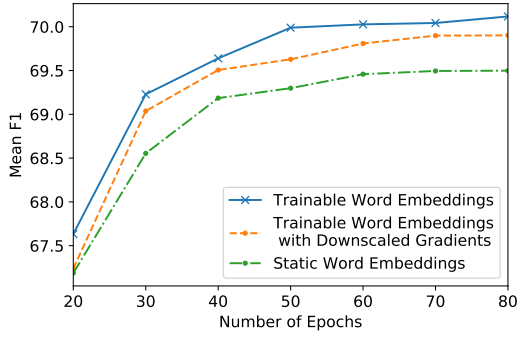


Figure 5: Mean F1-score (over 10 runs) on CoNLL04 development set with respect to number of training epochs for various embedding training strategies (without adversarial training or position embeddings).

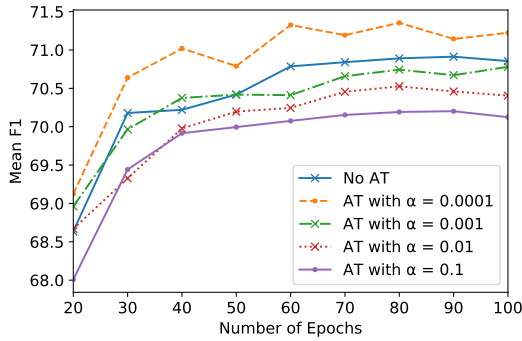


Figure 6: Mean F1 (over 10 runs) on CoNLL04 development set with respect to number of training epochs for values of α used in adversarial training.

tive using RMSProp (Tieleman and Hinton, 2012) with a relatively high initial learning rate of 0.005 given exponential decay is used.

Early experiments showed that, unlike models from prior work that used static word embeddings (Li et al., 2017; Bekoulis et al., 2018a), our model benefits from trainable word embeddings as shown in Figure 5. Here, trainable word embeddings with *downscaled* gradients refer to reducing the gradient of word embeddings by a factor of 10 at each training step. With regard to adversarial training, we find that it benefits the network marginally and only when trained on lower values of α as shown in Figure 6.

5 Results and Discussion

We report our main results in Tables 2 and 3 for the CoNLL04 and ADE datasets respectively. As a baseline, we replicate the prior best models (Bekoulis et al., 2018a) for both datasets based on publicly available source code². Unlike prior work, which reports performance based on a sin-

gle run, we report the 95% confidence interval around the mean F1 based on 30 runs with differing seed values for the CoNLL04 dataset. For the ADE dataset, we instead report the mean performance over 10-fold cross-validation so that results are comparable to established work. These experiments were performed using the same splits, pretrained embeddings, and computing hardware; hence, results are directly comparable.

We make the following observations based on our results from Table 2. Adversarial training (AT) only improves performance marginally, on average, and the improvements are not statistically significant. Both our model and the model from Bekoulis et al. (2018a) tend to skew heavily towards precision. However, our method with AT improves on both precision and recall, and by approximately 1% F1 on relation extraction where improvements are statistically significant ($p < 0.05$) based on the two-tailed Student’s t-test. We note that our model performs slightly worse when evaluated *purely* on NER. Based on Table 3, improvements from AT do not translate to the ADE dataset; instead, our method without AT performs marginally better in this case, improving over prior best result by almost 1% F1 for RE on average. While the prior best skews toward recall in this case, our method exhibits better balance of precision and recall. Finally, for our method, we observe that AT incurs an increase in training time but not in testing time. Based on run time results, we contend that our method is more computationally efficient given training and testing times are nearly four times lower than prior best efforts on either dataset. We note that dependency parsing accounts for more than half of our testing time (5 sec); using a more efficient parser with GPU support (SyntaxNet’s public binaries are CPU bound) may lead to even greater improvements in overall prediction speed. While training time may not be crucial in most settings, we argue that fast and efficient predictions are important for many end-user applications.

5.1 Ablation Analysis

We report ablation analysis results in Table 4 using our model with AT as the baseline. We note that the model hyperparameters were tuned on the CoNLL04 development set. As observed previously, improvements from AT did not generalize to the ADE dataset. Moreover, POS and character-based features had a negligible effect on perfor-

²https://github.com/bekou/multihead_joint_entity_relation_extraction

Model	Entity Recognition			Relation Extraction			Avg. Epoch	Avg.
	P (%)	R (%)	F (%)	P (%)	R (%)	F (%)	Training Time	Testing Time *
Table Representation(Miwa and Sasaki, 2014)	81.20	80.20	80.70	76.00	50.90	61.00	-	-
Multihead (Bekoulis et al., 2018b)	83.75	84.06	83.90	63.75	60.43	62.04	-	-
Multihead with AT (Bekoulis et al., 2018a)	-	-	83.61	-	-	61.95	-	-
Replicating Multihead with AT (Bekoulis et al., 2018a)†	84.36	85.80	85.07 ± 0.26	65.81	57.59	61.38 ± 0.50	614 sec	34 sec
Relation-Metric (Ours)†	83.97	84.33	84.38 ± 0.29	66.78	58.06	62.13 ± 0.43	101 sec	9 sec
Relation-Metric with AT (Ours)†	84.15	84.61	84.15 ± 0.26	67.24	58.04	62.29 ± 0.38	115 sec	9 sec

Table 2: Results comparing to other methods on the CoNLL04 dataset. We report 95% confidence intervals around the mean F1 over 30 runs for models appearing the last three rows.

†Results are directly comparable with the same train-test splits, pretrained word embeddings, and computing hardware.

*Average test time is per test set of 288 examples; dependency parsing accounts for about 5 seconds of our reported test time.

Model	Entity Recognition			Relation Extraction			Avg. Epoch	Avg.
	P (%)	R (%)	F (%)	P (%)	R (%)	F (%)	Training Time	Testing Time *
Neural Joint Model (Li et al., 2016)	79.50	79.60	79.50	64.00	62.90	63.40	-	-
Neural Joint Model (Li et al., 2017)	82.70	86.70	84.60	67.50	75.80	71.40	-	-
Multihead (Bekoulis et al., 2018b)	84.72	88.16	86.40	72.10	77.24	74.58	-	-
Multihead with AT (Bekoulis et al., 2018a)	-	-	86.73	-	-	75.52	-	-
Replicating Multihead with AT (Bekoulis et al., 2018a)†	85.76	88.17	86.95	74.43	78.45	76.36	1567 sec	40 sec
Relation-Metric (Ours)†	85.97	88.10	87.02	77.04	77.36	77.19	134 sec	9 sec
Relation-Metric with AT (Ours)†	85.84	88.08	86.94	76.59	77.30	76.94	169 sec	9 sec

Table 3: Results comparing to other methods on the ADE dataset. We report the mean performance over 10-fold cross-validation for models in the last three rows. Our models were tuned on the CoNLL04 development set based on hyperparameters from Table 1.

†Results are directly comparable with the same fixed 10-fold splits, pretrained word embeddings, and computing hardware.

*Average test time is per test set of 427 examples; dependency parsing accounts for about 5 seconds of our reported test time.

Model	Relation Extraction		
	P (%)	R (%)	F (%)
Full model	76.59	77.30	76.94
- Part-of-Speech Embeddings	77.00	77.58	77.27
- Character-based Input	77.12	77.36	77.23
- Adversarial Training	77.04	77.36	77.19
- Dependency Embeddings	76.51	77.22	76.85
- Position Embeddings	77.01	75.79	76.38
- Pretrained Word Embeddings	72.95	71.07	71.97

Table 4: Ablation studies based on 10-fold cross-validation over the ADE dataset; each row after the first indicates removal of a particular feature/component.

mance. On the other hand, dependency and position based features improved performance modestly, with position embeddings having a notable impact on recall. Unsurprisingly, pretrained word embeddings had the greatest impact on performance in terms of both precision and recall.

Comparison with More Prior Efforts. Gupta et al. (2016), Adel and Schütze (2017), and Zhang et al. (2017) also experimented with the CoNLL04 dataset; however, Gupta et al. (2016) evaluate on a more relaxed evaluation metric for matching entity bounds while Adel and Schütze (2017) assume entity bounds are known at test time thus treating the NER aspect as a simpler entity *classification*

problem. Of the three studies, results from Zhang et al. (2017) are most comparable given they consider entity bounds in their evaluations; however, their results are based on a *random* 80%–20% split of the train and test set. As we use established splits based on prior work, the two results are not directly comparable.

5.2 Error Analysis

Long sentences are a natural source of difficulty for relation extraction models given the potential for long-term dependencies. In this section, we perform simple error analysis by conducting experiments to assess model performance with respect to increasing sentence length. For this experiment, we train a single model using 80% of the dataset with 20% held out for testing. For some sentence length limit K , we evaluate on a subset of the overall test set that includes only examples with a sentence length that is less than or equal to K . Results from these experiments are plotted in Figures 7 and 8, for the CoNLL04 and ADE datasets respectively, such that K is varied along the horizontal x -axis. The top graph displays performance, while the bottom graph plots the number of examples with sentence length less

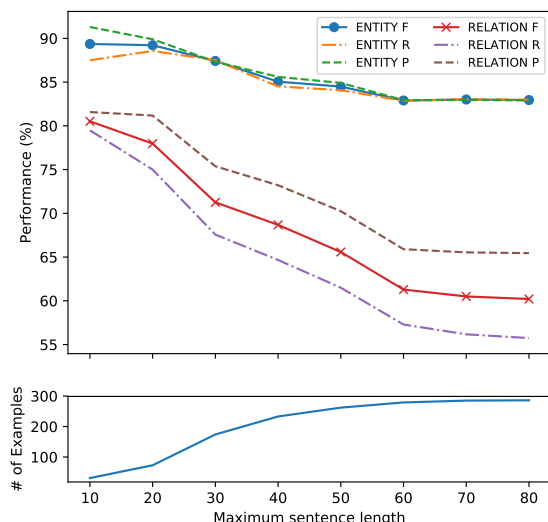


Figure 7: **CoNLL04**: Entity and relation extraction performance with respect to change in maximum sentence length. Experiments were performed using the original 80-20 training and testing split.

than or equal to K that are used for evaluation. As shown, performance on both NER and RE tend to decline as increasingly long sentences are added to the evaluation set. Unsurprisingly, relation extraction is more susceptible to long sentences compared to entity recognition. While there is a decline in both relation extraction precision and recall, we note that recall drops at a faster rate with respect to maximum sentence length and this phenomenon is apparent for both datasets. In future work, we will devise more effective ways of handling long sentences.

6 Conclusion

In this study, we introduced a novel neural architecture that combines the ideas of metric learning and convolutional neural networks to tackle the $\mathcal{E}2\mathcal{E}RE$ problem. Our method improved over the state-of-the-art with statistically significant results and substantially reduced training and testing times. Currently, the architecture is limited to *binary* relation extraction and intra-sentence relations; hence, future work will focus on handling *n*-ary relations and experimenting with document-level extraction involving cross-sentence relations.

References

Heike Adel and Hinrich Schütze. 2017. Global normalization of convolutional neural networks for joint entity and relation classification. In *Proceedings of the*

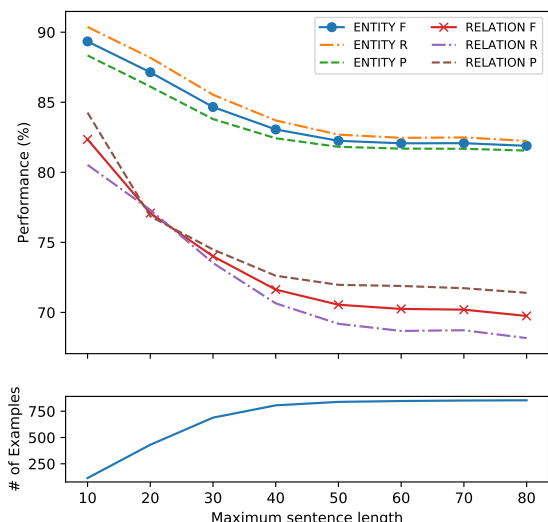


Figure 8: **ADE**: Entity and relation extraction performance with respect to change in maximum sentence length. Experiments were performed using a *random* 80-20 training and testing split.

2017 Conference on Empirical Methods in Natural Language Processing (EMNLP), pages 1723–1729.

Daniel Andor, Chris Alberti, David Weiss, Aliaksei Severyn, Alessandro Presta, Kuzman Ganchev, Slav Petrov, and Michael Collins. 2016. Globally normalized transition-based neural networks. *arXiv preprint arXiv:1603.06042*.

Giannis Bekoulis, Johannes Deleu, Thomas Demeester, and Chris Develder. 2018a. Adversarial training for multi-context joint entity and relation extraction. In *Proceedings of the 2018 Conference on Empirical Methods in Natural Language Processing (EMNLP)*, pages 2830–2836.

Giannis Bekoulis, Johannes Deleu, Thomas Demeester, and Chris Develder. 2018b. Joint entity recognition and relation extraction as a multi-head selection problem. *Expert Systems with Applications*, 114:34–45.

Jason PC Chiu and Eric Nichols. 2016. Named entity recognition with bidirectional LSTM-CNNs. *Transactions of the Association for Computational Linguistics*, 4:357–370.

Yejin Choi, Eric Breck, and Claire Cardie. 2006. Joint extraction of entities and relations for opinion recognition. In *Proceedings of the 2006 Conference on Empirical Methods in Natural Language Processing*, pages 431–439.

Michael Collins. 2002. Discriminative training methods for hidden markov models: Theory and experiments with perceptron algorithms. In *Proceedings of the ACL-02 conference on Empirical methods in natural language processing-Volume 10*, pages 1–8.

- Michael Goodfellow and Amanda L Jones. 2015. Laceyella. *Bergey's Manual of Systematics of Archaea and Bacteria*, pages 1–4.
- Pankaj Gupta, Hinrich Schütze, and Bernt Andrassy. 2016. Table filling multi-task recurrent neural network for joint entity and relation extraction. In *Proceedings of COLING 2016, the 26th International Conference on Computational Linguistics: Technical Papers*, pages 2537–2547.
- Harsha Gurulingappa, Abdul Mateen Rajput, Angus Roberts, Juliane Fluck, Martin Hofmann-Apitius, and Luca Toldo. 2012. Development of a benchmark corpus to support the automatic extraction of drug-related adverse effects from medical case reports. *Journal of biomedical informatics*, 45(5):885–892.
- Sergey Ioffe and Christian Szegedy. 2015. Batch normalization: Accelerating deep network training by reducing internal covariate shift. In *Proceedings of the 32nd International Conference on Machine Learning (ICML 2015)*, pages 448–456.
- Rohit J Kate and Raymond J Mooney. 2010. Joint entity and relation extraction using card-pyramid parsing. In *Proceedings of the Fourteenth Conference on Computational Natural Language Learning (CoNLL 2010)*, pages 203–212.
- Arzoo Katiyar and Claire Cardie. 2017. Going out on a limb: Joint extraction of entity mentions and relations without dependency trees. In *Proceedings of the 55th Annual Meeting of the Association for Computational Linguistics (Volume 1: Long Papers)*, volume 1, pages 917–928.
- J-D Kim, Tomoko Ohta, Yuka Tateisi, and Junichi Tsujii. 2003. Genia corpora semantically annotated corpus for bio-textmining. *Bioinformatics*, 19(suppl_1):i180–i182.
- Fei Li, Meishan Zhang, Guohong Fu, and Donghong Ji. 2017. A neural joint model for entity and relation extraction from biomedical text. *BMC bioinformatics*, 18(1):198.
- Fei Li, Yue Zhang, Meishan Zhang, and Donghong Ji. 2016. Joint models for extracting adverse drug events from biomedical text. In *Proceedings of the Twenty-Fifth International Joint Conference on Artificial Intelligence (IJCAI 2015)*, volume 2016, pages 2838–2844.
- Qi Li and Heng Ji. 2014. Incremental joint extraction of entity mentions and relations. In *Proceedings of the 52nd Annual Meeting of the Association for Computational Linguistics (Volume 1: Long Papers)*, volume 1, pages 402–412.
- Makoto Miwa and Mohit Bansal. 2016. End-to-end relation extraction using LSTMs on sequences and tree structures. In *Proceedings of the 54th Annual Meeting of the Association for Computational Linguistics (Volume 1: Long Papers)*, volume 1, pages 1105–1116.
- Makoto Miwa and Yutaka Sasaki. 2014. Modeling joint entity and relation extraction with table representation. In *Proceedings of the 2014 Conference on Empirical Methods in Natural Language Processing (EMNLP)*, pages 1858–1869.
- Sachin Pawar, Pushpak Bhattacharyya, and Girish Palshikar. 2017. End-to-end relation extraction using neural networks and markov logic networks. In *Proceedings of the 15th Conference of the European Chapter of the Association for Computational Linguistics: Volume 1, Long Papers*, volume 1, pages 818–827.
- Jeffrey Pennington, Richard Socher, and Christopher Manning. 2014. Glove: Global vectors for word representation. In *Proceedings of the 2014 conference on empirical methods in natural language processing (EMNLP)*, pages 1532–1543.
- Sampo Pyysalo, Filip Ginter, Hans Moen, Tapio Salakoski, and Sophia Ananiadou. 2013. Distributional semantics resources for biomedical text processing. In *Proceedings of 5th International Symposium on Languages in Biology and Medicine*, pages 39–44.
- Lev Ratinov and Dan Roth. 2009. Design challenges and misconceptions in named entity recognition. In *Proceedings of the Thirteenth Conference on Computational Natural Language Learning*, pages 147–155. Association for Computational Linguistics.
- Dan Roth and Wen-tau Yih. 2004. A linear programming formulation for global inference in natural language tasks. In *Proceedings of the Annual Conference on Computational Natural Language Learning (CoNLL)*, pages 1–8.
- Sameer Singh, Sebastian Riedel, Brian Martin, Jiaping Zheng, and Andrew McCallum. 2013. Joint inference of entities, relations, and coreference. In *Proceedings of the 2013 workshop on Automated knowledge base construction*, pages 1–6.
- Nitish Srivastava, Geoffrey Hinton, Alex Krizhevsky, Ilya Sutskever, and Ruslan Salakhutdinov. 2014. Dropout: A simple way to prevent neural networks from overfitting. *The Journal of Machine Learning Research*, 15(1):1929–1958.
- Tijmen Tieleman and Geoffrey Hinton. 2012. Lecture 6.5-rmsprop: Divide the gradient by a running average of its recent magnitude. *COURSERA: Neural Networks for Machine Learning*, 4(2).
- Bishan Yang and Claire Cardie. 2013. Joint inference for fine-grained opinion extraction. In *Proceedings of the 51st Annual Meeting of the Association for Computational Linguistics (Volume 1: Long Papers)*, volume 1, pages 1640–1649.
- Michihiro Yasunaga, Jungo Kasai, and Dragomir Radev. 2017. Robust multilingual part-of-speech tagging via adversarial training. In *Proceedings of the 16th Annual Conference of the North American*

Chapter of the Association for Computational Linguistics: Human Language Technologies.

- Xiaofeng Yu and Wai Lam. 2010. Jointly identifying entities and extracting relations in encyclopedia text via a graphical model approach. In *Proceedings of the 23rd International Conference on Computational Linguistics: Posters*, pages 1399–1407.
- Daniel Zeman, Martin Popel, Milan Straka, Jan Hajic, Joakim Nivre, Filip Ginter, Juhani Luotolahti, Sampo Pyysalo, Slav Petrov, Martin Potthast, Francis Tyers, Elena Badmaeva, Memduh Gokirmak, Anna Nedoluzhko, Silvie Cinkova, Jan Hajic jr., Jaroslava Hlavacova, Václava Kettnerová, Zdenka Uresova, Jenna Kanerva, Stina Ojala, Anna Missilä, Christopher D. Manning, Sebastian Schuster, Siva Reddy, Dima Taji, Nizar Habash, Herman Leung, Marie-Catherine de Marneffe, Manuela Sanguinetti, Maria Simi, Hiroshi Kanayama, Valeria de Paiva, Kira Droganova, Héctor Martínez Alonso, Çağr Çöltekin, Umut Sulubacak, Hans Uszkor-eit, Vivien Macketanz, Aljoscha Burchardt, Kim Harris, Katrin Marheinecke, Georg Rehm, Tolga Kayadelen, Mohammed Attia, Ali Elkahky, Zhuoran Yu, Emily Pitler, Saran Lertpradit, Michael Mandl, Jesse Kirchner, Hector Fernandez Alcalde, Jana Strnadová, Esha Banerjee, Ruli Manurung, Antonio Stella, Atsuko Shimada, Sookyoung Kwak, Gustavo Mendonca, Tatiana Lando, Rattima Nitisaroj, and Josie Li. 2018. Conll 2017 shared task: Multilingual parsing from raw text to universal dependencies. In *Proceedings of the CoNLL 2017 Shared Task: Multilingual Parsing from Raw Text to Universal Dependencies*, pages 1–19.
- Daojian Zeng, Kang Liu, Siwei Lai, Guangyou Zhou, Jun Zhao, et al. 2014. Relation classification via convolutional deep neural network. In *Proceedings of the 25th International Conference on Computational Linguistics: Technical Papers (COLING 2014)*, pages 2335–2344.
- Xiangrong Zeng, Daojian Zeng, Shizhu He, Kang Liu, and Jun Zhao. 2018. Extracting relational facts by an end-to-end neural model with copy mechanism. In *Proceedings of the 56th Annual Meeting of the Association for Computational Linguistics (Volume 1: Long Papers)*, volume 1, pages 506–514.
- Meishan Zhang, Yue Zhang, and Guohong Fu. 2017. End-to-end neural relation extraction with global optimization. In *Proceedings of the 2017 Conference on Empirical Methods in Natural Language Processing*, pages 1730–1740.
- Suncong Zheng, Yuexing Hao, Dongyuan Lu, Hongyun Bao, Jiaming Xu, Hongwei Hao, and Bo Xu. 2017a. Joint entity and relation extraction based on a hybrid neural network. *Neurocomputing*, 257:59–66.
- Suncong Zheng, Feng Wang, Hongyun Bao, Yuexing Hao, Peng Zhou, and Bo Xu. 2017b. Joint extraction of entities and relations based on a novel tagging scheme. In *Proceedings of the 55th Annual Meeting of the Association for Computational Linguistics (Volume 1: Long Papers)*, pages 1227–1236.